ACS central science

Research Article

http://pubs.acs.org/journal/acscii

Potent Human α-Amylase Inhibition by the β-Defensin-like Protein Helianthamide

Christina Tysoe,[†,#] Leslie K. Williams,[‡,#] Robert Keyzers,[§,∥] Nham T. Nguyen,[‡] Chris Tarling,[§] Jacqueline Wicki,[§] Ethan D. Goddard-Borger,[§] Adeleke H. Aguda,[‡] Suzanne Perry,[†] Leonard J. Foster,[†] Raymond J. Andersen,[§,∥] Gary D. Brayer,[‡] and Stephen G. Withers*[,†,‡,§]

[†]Centre for High-Throughput Biology, Michael Smith Laboratories, 185 East Mall, Vancouver, British Columbia V6T 1Z4, Canada
[‡]Department of Biochemistry and Molecular Biology, University of British Columbia, Vancouver, British Columbia V6T 1Z3, Canada
[§]Department of Chemistry, University of British Columbia, 2036 Main Mall, Vancouver, British Columbia V6T 1Z1, Canada
[∥]Department of Earth and Ocean Sciences, University of British Columbia, Vancouver, British Columbia V6T 1Z4, Canada

Supporting Information

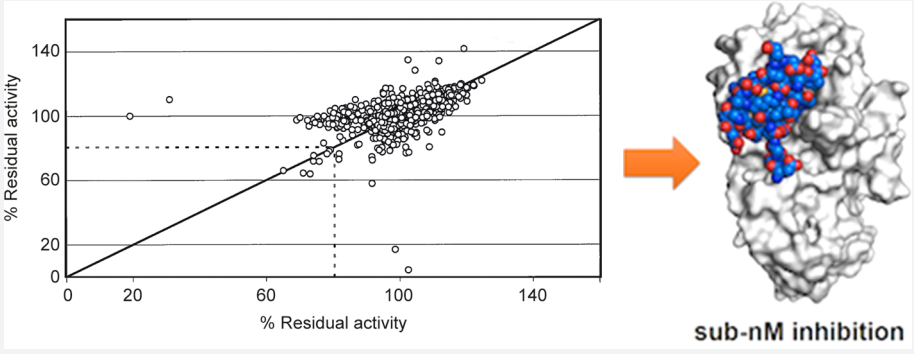

ABSTRACT: Selective inhibitors of human pancreatic α-amylase (HPA) are an effective means of controlling blood sugar levels in the management of diabetes. A high-throughput screen of marine natural product extracts led to the identification of a potent (K_i = 10 pM) peptidic HPA inhibitor, helianthamide, from the Caribbean sea anemone *Stichodactyla helianthus*. Active helianthamide was produced in *Escherichia coli* via secretion as a barnase fusion protein. X-ray crystallographic analysis of the complex of helianthamide with porcine pancreatic α-amylase revealed that helianthamide adopts a β-defensin fold and binds into and across the amylase active site, utilizing a contiguous YIYH inhibitory motif. Helianthamide represents the first of a novel class of glycosidase inhibitors and provides an unusual example of functional malleability of the β-defensin fold, which is rarely seen outside of its traditional role in antimicrobial peptides.

Diabetes mellitus is a metabolic disorder caused by the inability to produce adequate levels of insulin or effectively respond to the insulin being produced. This results in abnormally high blood glucose levels, which can lead to a number of serious consequences, including nerve and blood vessel damage, heart disease, kidney disease, stroke, and blindness.[1] Type II diabetes, in particular, has become increasingly common in the industrialized world and accounts for 90% of all diabetes cases.[2,3] Type II diabetes is the manifestation of pancreatic β-cell impairment and a gradual loss of cellular responsiveness to insulin. Since type II diabetes cases are associated with insulin insensitivity, and because high levels of insulin have been linked to obesity,[4] therapeutic interventions that act to lower blood glucose levels independently of this hormone are preferred. This can be accomplished by controlling the influx of glucose into the bloodstream from the liver (e.g., metformin) and the gastrointestinal tract (e.g., acarbose).[5]

The digestion of starch is a multistep process that begins in the oral cavity with the hydrolysis of insoluble starch polymers into shorter oligomers by salivary α-amylase.[6,7] Upon reaching the small intestine, pancreatic α-amylase provides a more extensive hydrolysis, cleaving the starch into a mixture of malto-oligosaccharides, primarily maltose and maltotriose. The resulting mixture then passes into the brush border of the small intestine where it is processed into glucose by the resident α-glucosidases maltase/glucoamylase and sucrase/isomaltase.[8] Most therapeutics currently in use are inhibitors of these α-glucosidases since this approach also prevented the hydrolysis of common dietary sugars such as sucrose into glucose while blocking the hydrolysis of starch-derived oligosaccharides.[9−11] The α-glucosidase inhibitors miglitol, voglibose, and acarbose are small molecule iminosugar-based

Received: December 23, 2015
Published: February 26, 2016

DOI: 10.1021/acscentsci.5b00399
ACS Cent. Sci. 2016, 2, 154−161

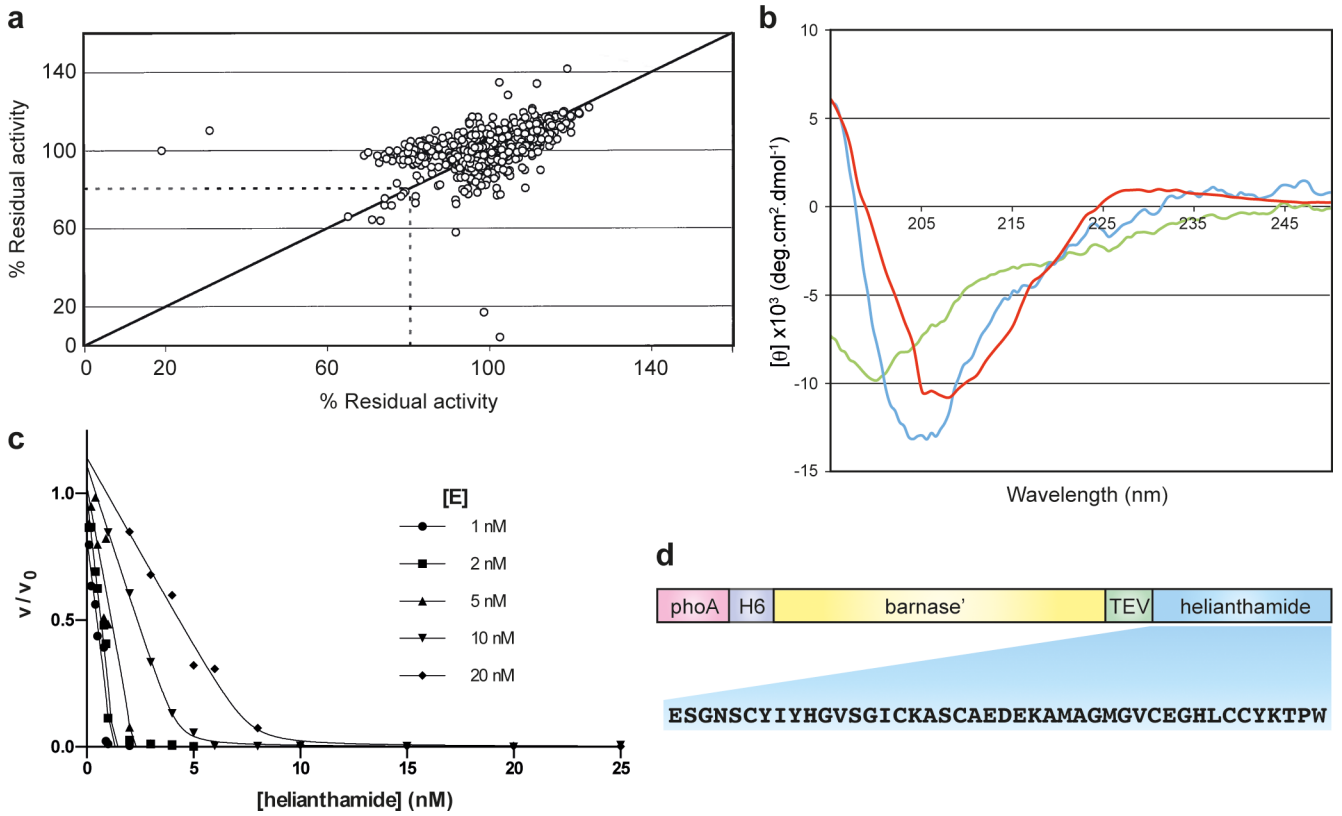

Figure 1. (a) Screening data from a high throughput screen designed for identification of HPA inhibitors. A total of 10 000 extracts from the UBC Marine Natural Products Library were tested as inhibitors of HPA. The screen was run in duplicate, and the relative activities measured in each well are plotted against the equivalent value for its duplicate as a single point. Crude extracts with ≤80% residual activity during both replicate screens (within the dashed box) were selected for further purification and analysis. (b) CD spectrophotometric analysis of natural (blue) and synthetic (green) and recombinant (red) helianthamide. (c) Kinetic analysis of recombinant helianthamide inhibition of HPA. Dose response curves of v/v_0 (observed rate over uninhibited rate) versus [helianthamide] were constructed for various enzyme concentrations at [CNP-G3] = 5 mM. The curves were fit to the Morrison equation of tight-binding inhibition (eq 1) via a least mean squares method to give values for the apparent inhibition constant, $K_{i,app}$, which were averaged and used to calculate K_i by eq 2, which is the relationship between these two values for competitive inhibitors. (d) Design of construct for recombinant expression.

inhibitors that have been used in the clinic, and unfortunately all are associated with deleterious side effects, ranging from diarrhea to hepatotoxicity.[12,13] While this is in part due to the natural consequences of displacement of di- and trisaccharides to the lower gut, which leads to osmotic-induced diarrhea and anaerobic fermentation, the problems are also due to systemic absorption and off-target activities.[14]

Human pancreatic α-amylase, which catalyzes the endohydrolysis of α(1−4)-D-glucosidic linkages in starch, represents a valuable therapeutic target within the starch degradation pathway, since intervention at this early point will minimize the aforementioned side effects. The enzyme is active within the lumen of the duodenum; thus, orally administered inhibitors that stay within the gastrointestinal tract will be optimally localized for amylase inhibition and will be less likely to cause undesirable side effects. Specific inhibition of this enzyme over the brush border α-glucosidases leads to the accumulation of longer chain carbohydrates in the lower gut, which do not produce the same osmotic effect seen with currently used therapeutics.[14,15] Since there is some evidence that specific inhibitors of amylases have evolved as antifeedants in nature,[16,17] we embarked upon a screen of natural product extracts with the expectation that this strategy would provide a good chance of yielding novel and potent amylase inhibitors.

RESULTS

High-Throughput Screening Uncovers a Novel Peptide Inhibitor of Human Pancreatic α-Amylase. A high-throughput, plate-based α-amylase assay utilizing the chromogenic substrate 2-chloro-4-nitrophenyl α-maltotrioside (CNPG3) was used to screen natural product extracts for novel HPA inhibitors. In this study, we explored the UBC Marine Natural Products Extract Library, which contains 10 000 natural product extracts of marine origin. Crude biological extracts can be advantageous over synthetic libraries as each sample contains a number of different primary and secondary metabolites, many of which are uncharacterized, enabling sampling of a large and diverse chemical space.

Samples were run in duplicate, and results of the screen are shown in Figure 1a. Crude extracts that resulted in ≤80% residual activity at a concentration of 5 μg/mL, indicated by the dotted lines in the plot, were selected for further analysis. The material with the greatest inhibitory activity was the product of exhaustive methanolic extraction of the Caribbean sea anemone *Stichodactyla helianthus*. Activity-guided extraction and purification involving successive runs of reversed-phase and size exclusion chromatography were performed to yield 2 mg of active material from a 154 g *S. helianthus* specimen.

^{1}H and ^{13}C NMR analysis indicated that the active component was proteinaceous in nature. Cleavage of the

DOI: 10.1021/acscentsci.5b00399
ACS Cent. Sci. 2016, 2, 154−161

reduced and iodoacetamide-treated protein with trypsin and GluC proteases followed by *de novo* LC/MS-MS and Edman sequencing yielded the following sequence (Figures S1 and S2), bearing six cysteine residues:

ESGNSCYIYHGVSGICKASCAEDEKAMAGMGVCEGH
LCCYKTPW

BLAST and PSI-BLAST analysis of this sequence revealed no significant homologues within the nonredundant protein sequence database. MALDI-TOF mass spectrometric analysis before (m/z = 4716.2) and after (m/z = 5066.6) treatment with dithiothreitol and iodoacetamide indicated the presence of three disulfide bridges. The protein, dubbed helianthamide (hel), was characterised by circular dichroism spectroscopy (Figure 1b and Table S1). The remaining material was used for preliminary inhibitory studies, in which reversible inhibition of HPA was observed with a low nanomolar inhibition constant.

Recombinant Expression of Helianthamide Provides a Practical Method for Producing Active Material. Having consumed the supply of active material extracted from *S. helianthus*, we pursued recombinant expression as a means of producing active helianthamide. We accomplished this via secretion from *Escherichia coli* using a barnase-based fusion system in which helianthamide was N-terminally fused to a hexahistidine-tagged inactive form of the bacterial ribonuclease (bar′) through a TEV protease cleavage site (Figure 1d). Barnase was selected as a fusion partner because of its lack of cysteines and propensity to spontaneously fold/refold—features that have proven useful in the expression of small disulfide-rich peptides in the past.[18] Incorporation of a N-terminal phoA signal peptide allowed for secretion of the bar′-hel fusion and utilization of the protein folding and disulfide-bond forming machinery of the bacterial SEC pathway.[19] A consequence of the TEV cleavage site is the addition of a Ser residue to the N-terminus of the helianthamide product after cleavage. As shown below, this is unlikely to impact the protein's inhibitory activity.

After some experimentation, we arrived at a quick, simple, and inexpensive expression and purification protocol that capitalized on the extraordinary stability of helianthamide. The protein was expressed in autoinduction media, the culture supernatant was collected and concentrated, and then purified by immobilized metal ion affinity chromatography (IMAC) in an average yield of 15 mg/L. Helianthamide was liberated from its fusion partner by the action of TEV protease. This reaction mixture was then diluted with an equal volume of methanol to precipitate all constituents except for helianthamide. Clarification of this solution returned helianthamide with >90% purity. This material was polished by reversed-phase HPLC to provide homogeneous protein. An average of 2 mg/L of helianthamide could be isolated after TEV cleavage and purification. A mass of 4771 Da was determined for recombinant helianthamide, which is the predicted mass of the peptide with oxidized cysteines. CD spectroscopy of the recombinant protein revealed a structure similar to that obtained for the material isolated from *S. helianthus* (Figure 1b and Table S1).

We turned to proteolysis and LC-MS/MS in an effort to establish the disulfide bond connectivity of the recombinant helianthamide. Attempts to perform controlled proteolysis on the peptide, with disulfides intact, were thwarted by the recalcitrance of helianthamide to the actions of trypsin, chymotrypsin, proteinase K, and Lys-C under all conditions trialed.[20] Attempts to make helianthamide more amenable to proteolysis by preincubation with cyanogen bromide or by partial reduction and alkylation of one or two disulfides were unsuccessful.[21] We resorted to performing a random acid hydrolysis of the peptide, an approach that complicates interpretation of resulting data sets.[22] A sample of recombinant helianthamide was incubated in 11 M HCl at 37 °C for 4 days, resulting in only partial digestion (as determined by HPLC). This partially digested material was analyzed by LC-MS/MS, leading to the identification of a series of signature peaks that, through collision-induced dissociation, enabled an assignment of disulfide connectivity (Figure S3 and Table S2). This data set indicated the connectivity of the disulfides to be in a 1−5, 2−4, 3−6 pattern (Figure S3).

Kinetic Analysis of Recombinant Helianthamide Suggests Highly Potent and Specific Inhibition of HPA. Since the helianthamide sample extracted from *S. helianthus* was predicted to be a low nanomolar inhibitor of HPA, kinetic analyses of recombinant helianthamide could not be pursued using conventional Michaelis−Menten methods.[23] Rather, inhibition constants were determined using the Morrison method in which inhibition dose response curves at [CNPG3] = K_M were constructed for varying enzyme concentrations.[24,25] The resulting data (Figure 1c) were fit to the Morrison equation (eq 1) to determine the apparent inhibition constant, $K_{i\text{-app}}$. $K_{i\text{-app}}$ can be converted to K_i through eq 2, which is the relationship between these values for competitive inhibition.[24] Using this method, recombinant helianthamide was determined to have a K_i of 0.01 nM against HPA. The bar'-hel fusion was also shown to be a potent inhibitor of HPA and inhibited the enzyme with a K_i of 0.5 nM, 50-fold weaker than free helianthamide.

$$v = v_o\left(1 - ([E]_0 + [I] + K_{i\text{-app}}) - \frac{\sqrt{([E]_0 + [I] + K_{i\text{-app}})^2 - 4[E]_0[I]}}{2[E]_0}\right) \quad (1)$$

$$K_{i\text{-app}} = K_i\left(1 + \frac{[S]}{K_M}\right) \quad (2)$$

The specificity of helianthamide was investigated by testing for inhibition of 10 other glycosidases, including a human intestinal α-glucosidase and two bacterial α-amylases that are common in the gut microbiome (Table S3). Only porcine pancreatic α-amylase (PPA) was inhibited (K_i = 0.1 nM), suggesting that helianthamide is highly selective for mammalian amylases.

Pancreatic α-Amylase Allows for Templated Folding of Linear, Reduced Helianthamide To Yield a Crystal Structure of the Helianthamide/Amylase Complex. Repeated attempts to cocrystallize HPA with recombinant helianthamide for X-ray crystallographic analysis were unsuccessful, most likely due to the occluded nature of the active site of HPA in its dominant crystal form. We therefore turned our attention to porcine pancreatic α-amylase (PPA), which has high sequence and structural homology to HPA,[26] but has a more accessible active site than the human isozyme in the crystalline state. We also explored the use of a reduced (linear) helianthamide, produced by chemical synthesis, with hopes that

DOI: 10.1021/acscentsci.5b00399
ACS Cent. Sci. 2016, 2, 154−161

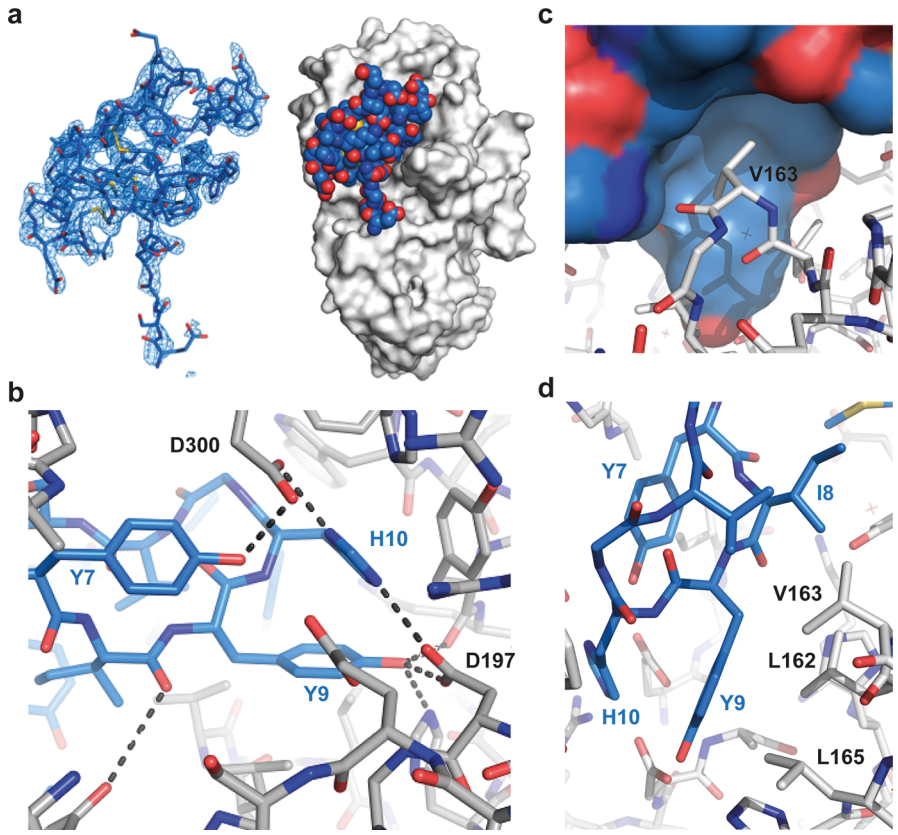

Figure 2. Crystal structure of helianthamide and PPA. (a) Helianthamide (blue and red spheres) is observed within the active site cleft of PPA, based on its fit to the corresponding electron density map of its structure. (b) A view of the complexed structure providing a closer examination of the amylase active site (gray) that reveals three residues of helianthamide (blue), Y7, Y9, and H10, interacting with key residues of PPA. (c) Hydrophobic interactions play a large part in helianthamide binding. A large hydrophobic pocket of helianthamide (blue, surface) is observed around V163 of PPA (gray, stick), adjacent to the enzyme active site. (d) Another view of the amylase active site with an emphasis on hydrophobic interactions. In particular, I8 and V12 interact with the hydrophobic ridges surrounding the amylase active site. The coordinates for the helianthamide/PPA complex structure have been deposited in the Protein Data Bank (4X0N).

the crystalline amylase would allow the more flexible ligand into its active site and subsequently template its folding. Crystallization trials with PPA and the synthetic helianthamide yielded crystals of the helianthamide/PPA complex which grew via the hanging drop method in approximately 3 weeks. X-ray diffraction data collected for these samples were processed into a structural model with a 2.6 Å resolution (Table S4).

This structure (Figure 2) displays helianthamide bound in a noncovalent complex with PPA. A third of helianthamide's solvent accessible surface area is buried in contact with PPA, primarily within and around the amylase active site. Helianthamide is composed of a four-stranded antiparallel β-sheet with three disulfide bonds connected with the same 1−5, 2−4, 3−6 topology that was determined for recombinant helianthamide. Within the amylase active site, three residues of helianthamide, Tyr7, Tyr9, and His10, interact with PPA's catalytic residues. Both Tyr9 and His10 hydrogen bond to the enzyme's catalytic nucleophile residue, Asp197.[27] Tyr9 also forms hydrogen bonds with His101 and Tyr62, which border the active site of the enzyme. His10 forms a second hydrogen bond to Asp300, a residue that coordinates the substrate 2- and 3-hydroxyls in the −1 subsite and helps position water during catalysis. Sitting further back within the active site, Tyr7 also hydrogen bonds to Asp300. A hydrogen bond between the main chain carbonyl of Ile8 and the enzyme's Tyr151 rounds out the polar interactions in the active site of PPA. There are no direct interactions with the acid/base catalyst Glu233.

Outside the amylase active site there are relatively few hydrogen bonds or ionic interactions between helianthamide and PPA. Residues Ser2, Ser5, and Ser13 of helianthamide form hydrogen bonds with residues 305, 308, and 310 of the enzyme. Ala28 and Trp44 also form polar contacts with the enzyme. The N-terminus of helianthamide protrudes into solution (Figure S4), supporting the notion that the additional N-terminal Ser of the recombinant material should not disrupt any interactions with the enzyme—if anything it could contribute to new polar contacts. A hydrophobic interface is observed between helianthamide and PPA near the amylase active site. Hydrophobic patches around the pancreatic α-amylase active site cleft have been noted previously and were shown to position and stabilize the amylose substrate.[28] Helianthamide is able to interact with these patches through its own hydrophobic residues, one of them being Ile8, which orients its side chain in the opposite direction of the adjacent residues, Tyr7 and Tyr9. Ile8, along with Val12, contributes to helianthamide's hydrophobic surface area, which appears to form a pocket around Val163 of PPA (Figure 2c,d).

DISCUSSION

Although BLAST searches revealed no known sequence-based homologues of helianthamide, structural searches with DALI revealed helianthamide to be structurally homologous to the β-defensins (Figure 3). The β-defensins are a family of

DOI: 10.1021/acscentsci.5b00399
ACS Cent. Sci. 2016, 2, 154−161

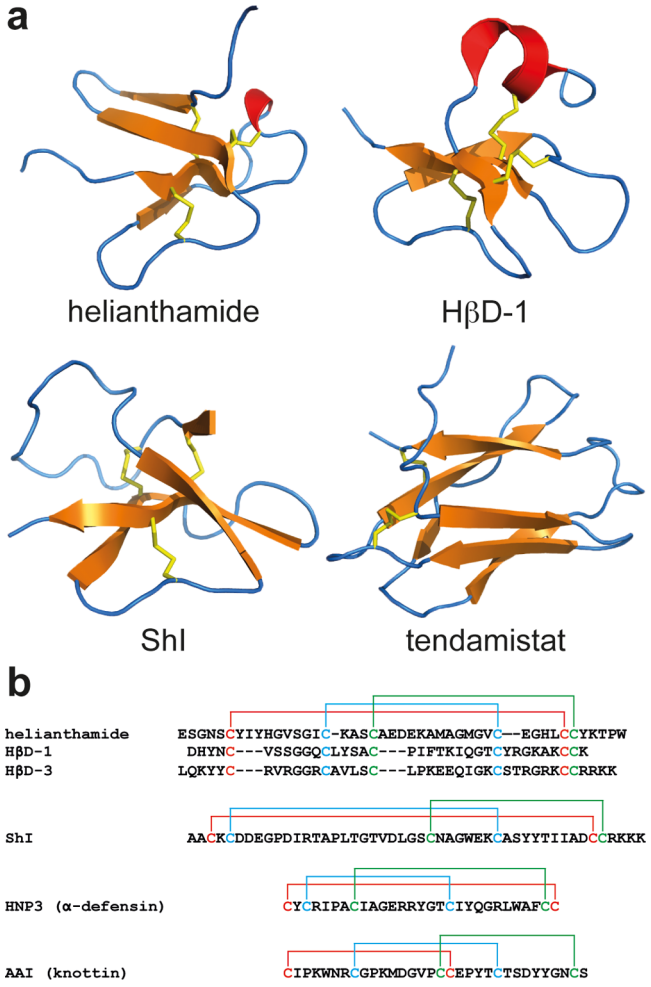

Figure 3. Structural and sequence comparisons of helianthamide with other disulfide rich peptides. (a) Structural comparison of helianthamide to the human β-defensins (hβD-1 as a representative) (PDB: 2NLS), ShI (PDB: 1SH1), and tendamistat (PDB: 1BVN). β-sheets depicted in orange, helices in red, loops in blue, and disulfide bonds in yellow. (b) Sequence alignment of helianthamide with two β-defensins, and comparisons to ShI, and representatives from the α-defensin and knottin families. Disulfide connectivities are color coded where bonding partners share the same color.

mammalian and avian antimicrobial peptides characterized by their cationic and amphipathic nature, 1−5, 2−4, 3−6 disulfide topology, and antiparallel β-sheet core.[29,30] While rare, structural homologues of the β-defensins have been uncovered in the past. To date, all known non-antibiotic homologues are potent toxins that inhibit sodium or potassium ion channels.[31] One such toxin, ShI, was also isolated from *Stichodactyla helianthus*.[32] In the case of the β-defensins and their toxic structural relatives, charge distribution on the peptide surface is required for their fatal activities. Helianthamide does not emulate its relatives in this regard. Rather, its helianthamide's neutral residues that make it unique in yet another regard and contribute to its incredible potency.

There are several well-studied examples of peptidic amylase inhibitors, which are common in many different plant species as a defense against grazing pressures. Some of these peptides have evolved as specific inhibitors of a particular predator's α-amylase, while others have been developed with a dual function, such as accompanying protease inhibition. The amaranth amylase inhibitor (AAI) (Figure 3b) is a 32-residue knottin peptide, which specifically inhibits mealworm α-amylase by blocking four substrate-binding subsites. Contact with the enzyme's catalytic residues is minimal and mediated by a single arginine residue.[33] Unlike that of the β-defensins, the knottin fold, with its 1−4, 2−5, 3−6 disulfide topology, is a diverse scaffold with many known applications in nature.

While most peptidic amylase inhibitors are from higher plants, the most potent known inhibitor of HPA, tendamistat, is a peptide from *Streptomyces tendae*. Tendamistat is a 74-residue peptide with two disulfide bonds. The inhibitor forms polar contacts with HPA over four discontinuous regions of the peptide sequence; however, interactions with the enzyme's catalytic machinery occur through a single arginine residue positioned on the tip of a disulfide stabilized β-turn.[33] Helianthamide, with a K_i of 10 pM, is now possibly the most potent human α-amylase inhibitor discovered to date. At the very least it equals the potency of tendamistat (K_i estimated at 9−200 pM).[33−35] Tendamistat was pursued as a therapeutic agent and was shown to cause a significant decrease in blood plasma glucose levels during clinical trials.[36] However, its vulnerability to degradation and pronounced immunogenicity, thought to be due to its β-sandwich fold that resembles T-cell receptors (Figure 3a), quickly led to its abandonment in the clinic.[16,35,37] Helianthamide represents a new platform for the clinical inhibition of HPA. It has equal or greater potency than tendamistat and possesses unrivalled structural stability as a result of its β-defensin fold. This structural feature may obviate the immunogenicity problems encountered for tendamistat. Perhaps most importantly, helianthamide is resistant to proteolytic degradation, prolonged exposure to low pH, and high temperature, suggesting that it would be suitable for oral administration.

Our structural analysis demonstrates that three aromatic residues of helianthamide (Tyr7, Tyr9, and His10) make all of the important polar contacts with the catalytic machinery of PPA. They flank an isoleucine that, along with Val12, creates a nonpolar interface to complement the hydrophobic ridges bordering PPA's active site. This contiguous YIYH motif of helianthamide may hold potential as a pharmacophore in its own right.

Aspects of the YIYH inhibitory motif mirror another natural product recently identified as an HPA inhibitor. Montbretin A (MbA), a complex flavonol glycoside derivative from the *Crocosmia* plant family, was discovered in a screen of terrestrial plant extracts and has a K_i of 8 nM against HPA.[17] The root of MbA's inhibitory activity was traced to a core structure containing myricetin and caffeic acid linked by a disaccharide.[38] The phenolic moieties were shown to be essential for inhibition and interact directly with the conserved active site carboxylic acids. An overlay of the bound structure of MbA (PDB: 4W93) with the inhibitory motif of helianthamide reveals a strikingly similar orientation of the inhibitory moieties (Figure 4). Tyr9 of helianthamide aligns with MbA's A-ring; their hydroxyl groups line up to both interact with the catalytic nucleophile, Asp197 of amylase. His10 is positioned similarly to the caffeic ester moiety, though in an almost perpendicular orientation, with Asp300 of the enzyme orienting its side chain inward to interact with the imidazole ring. This confluence of inhibitory motifs from remote natural sources points to a very promising pharmacophore for specific inhibition of amylases. Conversely, an overlay of the helianthamide inhibitory motif with the structure of the general α-glucosidase inhibitor acarbose results

DOI: 10.1021/acscentsci.5b00399
ACS Cent. Sci. 2016, 2, 154−161

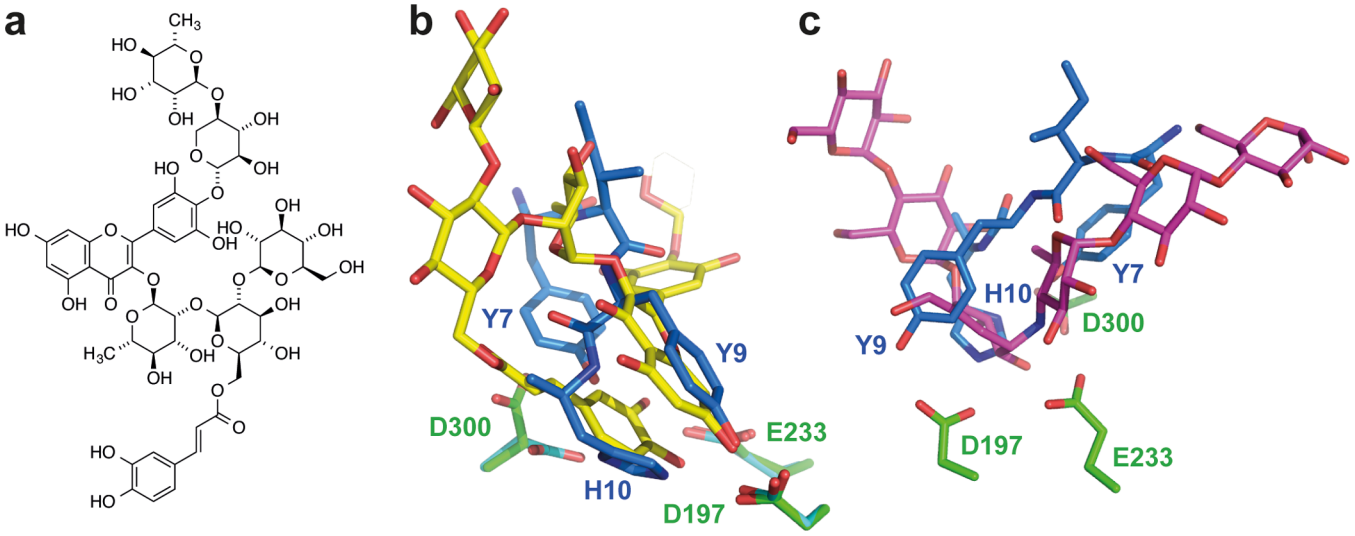

Figure 4. Comparison of helianthamide with montbretin A and acarbose as HPA inhibitors. (a) Structure of montbretin A; (b) overlay of helianthamide's inhibitory motif (blue) with montbretin A (yellow) (PDB: 4W93); (c) Overlay of helianthamide's inhibitory motif (blue) with an extended derivative of acarbose resulting from enzyme-mediated rearrangement[41] (pink) (PDB: 1XH0).

in very little overlap of functional groups (Figure 4c). Indeed, unlike acarbose, MbA and helianthamide do not mimic the oligosaccharide substrate in structure or binding, which likely plays a role in their specificity against α-amylase.

CONCLUSION

Helianthamide represents a unique and novel class of mammalian α-amylase inhibitors with many valuable features that make it a lead structure for preclinical development. This peptide exhibits the highest level of amylase inhibition yet observed in nature, appears to be specific for mammalian pancreatic α-amylase over other glycosidases, is easy to manufacture in high yields from *E. coli*, and possesses a novel YIYH inhibitory motif that may serve as inspiration for further drug development. While peptide therapeutics are not typically considered as a means of controlling postprandial blood glucose levels, due to their vulnerability to hydrolysis in the digestive system, the impressive stability of helianthamide, arising from its tightly knotted disulfide-rich core, renders it a promising candidate for oral delivery.[39] Additionally, the inherently low bioavailability of proteins could serve to prevent systemic absorption and minimize side effects, such as those observed for small molecule glycosidase inhibitors.

MATERIALS AND METHODS

High-Throughput Screening. Screening was performed on a Beckman Coulter Biomek FX Laboratory Automation Workstation (Fullerton, CA, USA) integrated with a Beckman Coulter DTX880 plate reader with UV/Vis capability. The screening assay was run in 384-well plates containing a 60 μL volume of 50 mM sodium phosphate, 100 mM sodium chloride buffer (pH 7.0), HPA (1 μg mL^{-1}), and the commercially available HPA substrate 2-chloro-4-nitrophenyl α-maltotrioside (1 mM; K_M = 3.6 mM). Triton X-100 (0.01%) was included to minimize detection of nonspecific inhibitors. The natural product extract samples were present as DMSO solutions that contained 5 mg mL^{-1} of dried methanolic extract, which were tested at a dilution of 60 nL in a final assay volume of 60 μL. HPA was found to be unaffected by the addition of this small amount of DMSO (0.1%) and Triton X-100 (0.01%). The integrity of the assay was tested through the use of two test plates run as the first and last plate of each batch and which contained a serial dilution of the known HPA inhibitor acarbose. Validation of hits from the primary screen was performed manually on a UV/Vis spectrophotometer. Among the hits examined in this secondary screen, the natural extract from the sea anemone *Stoichactis helianthus* proved to have the highest activity against HPA. A more detailed account of the screening methodology used can be found in Tarling et al. 2008.[17]

Cloning and Recombinant Expression of the Helianthamide. A synthetic gene of the desired construct was ordered as a pUC-57 plasmid from BioBasic Canada. The gene was subcloned into a pET-29b+ vector and single clones were sequenced to verify correct ORF. The desired plasmid was transformed into electrocompetent BL21* *E. coli*, which were screened on Luria–Bertani agarose plates containing 50 μg/mL kanamycin. Starter cultures were made by incubating colonies containing the desired plasmid in 5 mL of LB medium containing 50 μg/mL kanamycin overnight at 37 °C. Starter cultures were added to 500 mL of LBE-5052 autoinduction media.[40] The expression cultures were incubated at 25 °C (230 rpm) for 24 h. The resulting culture supernatant was treated with 60% ammonium sulfate. The ammonium sulfate solution was stirred at 4 °C for 1 h before centrifugation to isolate the precipitated proteins. The proteins were resuspended in His-trap binding buffer (20 mM sodium phosphate, 500 mM sodium chloride, 5 mM imidazole, pH 8) and applied to a Ni-NTA agarose column. The protein of interest was eluted over a gradient of increasing imidazole. The crude fusion was then cleaved using 100 units of TurboTEV protease (Accelagen) per milligram of fusion at 30 °C for 16 h. Helianthamide was purified from the reaction mixture by addition of an equal volume of methanol, leading to precipitation of TEV protease, bar′, and remaining uncleaved bar′-hel. For production of the fusion mutants, site-directed mutagenesis was performed via the four-primer method.[42] The mutated genes were ligated into pET-29b+ plasmids and transformed into BL21* *E. coli*. Expression conditions and purification were the same as for the wild-type fusion.

DOI: 10.1021/acscentsci.5b00399
ACS Cent. Sci. 2016, 2, 154–161

Kinetic Analysis of Recombinant Material. All commercial enzymes were purchased from Sigma-Aldrich. Assays were performed on a Varian Cary 300 UV/vis spectrophotometer. The release of 2-chloro-4-nitrophenol resulting from the amylase catalyzed hydrolysis of 2-chloro-4-nitrophenyl α-maltotrioside was monitored at 400 nm. Reactions were run at 30 °C in 50 mM sodium phosphate, 100 mM sodium chloride (pH 7.0). Reactions were monitored over 5 min to measure the initial reaction rate. For K_i values less than 50 nM, inhibition constants were calculated using the Morrison equation for tight-binding inhibition. Reactions were run with a final [CNPG3] = 5 mM. Typically six different inhibitor concentrations were used for each enzyme concentration. Up to five different enzyme concentrations were used, ranging from 1 nM to 10 nM. v/v_0 was plotted against [I] for each enzyme concentration to form a series of dose response curves. These data sets were then fitted to the Morrison equation using a least mean squares method to determine a value of $K_{i\text{-}app}$ for each enzyme concentration. $K_{i\text{-}app}$ was then used to calculate K_i. K_i values greater than 50 nM were determined by Michaelis−Menten inhibition kinetics. Details of this process can be found in the work done by Tarling et al.[17] After kinetic analysis with HPA, nine additional enzymes were tested against helianthamide. Concentrations of up to 1 μM of helianthamide were used to assess for inhibition.

Crystallization of Synthetic Helianthamide/PPA Complex. Synthetic peptide was purchased from AnaSpec Inc. Porcine pancreatic α-amylase (PPA) was purchased from Sigma (A4268). The crystallization conditions used were based on the Hampton Research Crystal Screen kit. Diffraction quality crystals of PPA-helianthamide were grown by combining PPA and synthetic linear helianthamide in a 1:2.5 enzyme/inhibitor molar ratio. Two microliters of the enzyme inhibitor solution was mixed with 2 μL of 100 mM Tris, pH 8.5, 8% PEG-8000 (mother liquor) on siliconized microscope slides. The slides were inverted and sealed over wells containing 500 μL of mother liquor. The crystals grew at room temperature over a period of approximately 3 weeks. The crystals were soaked in mother liquor with 30% glycerol before flash freezing in liquid nitrogen and sent to Stanford Synchrotron Radiation Lightsource for remote data collection.

X-ray Crystallographic Data Collection, Processing, and Refinement. Data were collected using a MarMosaic 325 CCD detector on beamline 9-2 at the SSRL using a wavelength of 0.9794 Å and a 1° oscillation. The resulting data were processed using Mosflm and were scaled, merged, and truncated using Scala. Molecular replacement was performed using CNS. The coordinates of PPA [PDB ID: 1PIF] were used for the model from which the initial phases were derived. The coordinates for helianthamide were built in manually into the empty density of the amylase active site using Coot based on the sequence of the peptide.

■ ASSOCIATED CONTENT

Ⓢ Supporting Information

. The Supporting Information is available free of charge on the ACS Publications website at DOI: 10.1021/acscentsci.5b00399.

Materials and methods, MS/MS data, gene and protein sequences, inhibition specificity studies, X-ray crystallography structure determination statistics, Figures S1−S7, and Tables S1−S4 (PDF)

■ AUTHOR INFORMATION

Corresponding Author

*Tel. 604 822 3402 E-mail: withers@chem.ubc.ca.

Author Contributions

#C.T. and L.K.W. contributed equally.

Notes

The authors declare the following competing financial interest(s): A patent on the use of helianthamide for amylase inhibition and blood glucose control has been submitted by the University of British Columbia with some of the authors named as inventors.

■ ACKNOWLEDGMENTS

We would like to thank Jason Rogalski of the UBC Proteomics Core Facility for his help with *de novo* sequencing and subsequent mass spectrometric analysis of helianthamide; Dr. William Walters for writing a script for the processing and analysis of LC-MS/MS data; Emily Kwan for supplying the wild-type HPA used in this study; Dr. David R. Rose for supplying mammalian intestinal α-glucosidases; Dr. Emily Schlenz, University of Sao Paulo, for taxonomic identification of the sea anemone; and Dr. France Dumas, NRC Biotechnology Institute, for performing the Edman sequencing. This work was supported by an operating grant from the Canadian Institutes of Health Research (CIHR - Reference Numbers (FRN): 111082, (to G.D.B. and S.G.W.)) and an operating grant from the Natural Sciences and Engineering Research Council of Canada (NSERC) to R.J.A. L.K.W. was supported by an Alexander Graham Bell Canada Graduate Scholarship (NSERC). S.G.W. is supported by a Tier 1 Canada Research Chair. Portions of this research were carried out at the Stanford Synchrotron Radiation Lightsource, SLAC National Accelerator Laboratory, which is supported by the U.S. Department of Energy, Office of Science, Office of Basic Energy Sciences under Contract No. DE-AC02-76SF00515. The SSRL Structural Molecular Biology Program is supported by the DOE Office of Biological and Environmental Research, and by the National Institutes of Health, National Institute of General Medical Sciences (including P41GM103393). The contents of this publication are solely the responsibility of the authors and do not necessarily represent the official views of NIGMS or NIH. The graphics program PyMol was used in part to generate figures.

■ REFERENCES

(1) Adeghate, E.; Schattner, P.; Dunn, E. An update on the etiology and epidemiology of diabetes mellitus. *Ann. N. Y. Acad. Sci.* **2006**, *1084*, 1−29.

(2) Aye, T.; Levitsky, L. L. Type 2 diabetes: an epidemic disease in childhood. *Curr. Opin. Pediatr.* **2003**, *15*, 411−415.

(3) Smyth, S.; Heron, A. Diabetes and obesity: the twin epidemics. *Nat. Med.* **2006**, *12*, 75−80.

(4) Lee, Y.; Berglund, E. D.; Yu, X.; Wang, M. Y.; Evans, M. R.; Scherer, P. E.; Holland, W. L.; Charron, M. J.; Roth, M. G.; Unger, R. H. Hyperglycemia in rodent models of type 2 diabetes requires insulin-resistant alpha cells. *Proc. Natl. Acad. Sci. U. S. A.* **2014**, *111*, 13217−13222.

(5) Inzucchi, S. E.; Bergenstal, R. M.; Buse, J. B.; Diamant, M.; Ferrannini, E.; Nauck, M.; Peters, A. L.; Tsapas, A.; Wender, R.; Matthews, D. R. Management of hyperglycaemia in type 2 diabetes, 2015: a patient-centred approach. Update to a position statement of the American Diabetes Association and the European Association for the Study of Diabetes. *Diabetologia* **2015**, *58*, 429−442.

DOI: 10.1021/acscentsci.5b00399
ACS Cent. Sci. 2016, 2, 154−161

(6) Ramasubbu, N.; Paloth, V.; Luo, Y.; Brayer, G. D.; Levine, M. J. Structure of human salivary alpha-amylase at 1.6 A resolution: implications for its role in the oral cavity. *Acta Crystallogr., Sect. D: Biol. Crystallogr.* **1996**, *52*, 435−446.
(7) Butterworth, P. J.; Warren, F. J.; Ellis, P. R. Human alpha-amylase and starch digestion: An interesting marriage. *Starch Journal* **2011**, *63*, 395−405.
(8) Nichols, B. L.; Avery, S.; Sen, P.; Swallow, D. M.; Hahn, D.; Sterchi, E. The maltase-glucoamylase gene: common ancestry to sucrase-isomaltase with complementary starch digestion activities. *Proc. Natl. Acad. Sci. U. S. A.* **2003**, *100*, 1432−1437.
(9) Sels, J. P.; Huijberts, M. S.; Wolffenbuttel, B. H. Miglitol, a new alpha-glucosidase inhibitor. *Expert Opin. Pharmacother.* **1999**, *1*, 149−156.
(10) van de Laar, F. A. Alpha-glucosidase inhibitors in the early treatment of type 2 diabetes. *Vasc. Health Risk Manag.* **2008**, *4*, 1189−1195.
(11) Baron, A. D. Postprandial hyperglycaemia and alpha-glucosidase inhibitors. *Diabetes Res. Clin. Pract.* **1998**, *40* (Suppl), S51−S55.
(12) Hsiao, S. H.; Liao, L. H.; Cheng, P. N.; Wu, T. J. Hepatotoxicity associated with acarbose therapy. *Ann. Pharmacother.* **2005**, *40*, 151−154.
(13) Vichayanrat, A.; Ploybutr, S.; Tunlakit, M.; Watanakejorn, P. Efficacy and safety of voglibose in comparison with acarbose in type 2 diabetic patients. *Diabetes Res. Clin. Pract.* **2002**, *55*, 99−103.
(14) Boivin, M.; Flourie, B.; Rizza, R. A.; Go, V. L.; DiMagno, E. P. Gastrointestinal and metabolic effects of amylase inhibition in diabetics. *Gastroenterology* **1988**, *94*, 387−394.
(15) Boivin, M.; Zinsmeister, A. R.; Go, V. L.; DiMagno, E. P. Effect of a purified amylase inhibitor on carbohydrate metabolism after a mixed meal in healthy humans. *Mayo Clin. Proc.* **1987**, *62*, 249−255.
(16) Gonçalves, O.; Dintinger, T.; Blanchard, D.; Tellier, C. Functional mimicry between anti-Tendamistat antibodies and alpha-amylase. *J. Immunol. Methods* **2002**, *269*, 29−37.
(17) Tarling, C. A.; Woods, K.; Zhang, R.; Brastianos, H. C.; Brayer, G. D.; Andersen, R. J.; Withers, S. G. The search for novel human pancreatic alpha-amylase inhibitors: high-throughput screening of terrestrial and marine natural product extracts. *ChemBioChem* **2008**, *9*, 433−438.
(18) Schmoldt, H.-U.; Wentzel, A.; Becker, S.; Kolmar, H. A fusion protein system for the recombinant production of short disulfide bond rich cystine knot peptides using barnase as a purification handle. *Protein Expression Purif.* **2005**, *39*, 82−89.
(19) Hoffman, C. S.; Wright, A. Fusions of secreted proteins to alkaline phosphatase: an approach for studying protein secretion. *Proc. Natl. Acad. Sci. U. S. A.* **1985**, *82*, 5107−5111.
(20) Tang, Y. Q.; Selsted, M. E. Characterization of the disulfide motif in BNBD-12, an antimicrobial beta-defensin peptide from bovine neutrophils. *J. Biol. Chem.* **1993**, *268*, 6649−6653.
(21) Schroeder, B. O.; Wu, Z.; Nuding, S.; Groscurth, S.; Marcinowski, M.; Beisner, J.; Buchner, J.; Schaller, M.; Stange, E. F.; Wehkamp, J. Reduction of disulphide bonds unmasks potent antimicrobial activity of human β-defensin 1. *Nature* **2011**, *469*, 419−423.
(22) Bauer, M.; Sun, Y.; Degenhardt, C.; Kozikowski, B. Assignment of all four disulfide bridges in echistatin. *J. Protein Chem.* **1993**, *12*, 759−764.
(23) Copeland, R. A. *Enzymes: A Practical Introduction to Structure, Mechanism, and Data Analysis*, 2nd ed.; Wiley-VCH: New York, 2002.
(24) Morrison, J. F. Kinetics of the reversible inhibition of enzyme-catalysed reactions by tight-binding inhibitors. *Biochim. Biophys. Acta* **1969**, *185*, 269−286.
(25) Murphy, D. J. Determination of accurate *K*I values for tight-binding enzyme inhibitors: an in silico study of experimental error and assay design. *Anal. Biochem.* **2004**, *327*, 61−67.
(26) Brayer, G. D.; Luo, Y.; Withers, S. G. The structure of human pancreatic alpha-amylase at 1.8 A resolution and comparisons with related enzymes. *Protein Sci.* **1995**, *4*, 1730−1742.
(27) Rydberg, E. H.; Li, C.; Maurus, R.; Overall, C. M.; Brayer, G. D.; Withers, S. G. Mechanistic analyses of catalysis in human pancreatic alpha-amylase: detailed kinetic and structural studies of mutants of three conserved carboxylic acids. *Biochemistry* **2002**, *41*, 4492−4502.
(28) Qian, M.; Spinelli, S.; Driguez, H.; Payan, F. Structure of a pancreatic alpha-amylase bound to a substrate analogue at 2.03 A resolution. *Protein Sci.* **1997**, *6*, 2285−2296.
(29) White, S. H.; Wimley, W. C.; Selsted, M. E. Structure, function, and membrane integration of defensins. *Curr. Opin. Struct. Biol.* **1995**, *5*, 521−527.
(30) Ganz, T. Defensins: antimicrobial peptides of innate immunity. *Nat. Rev. Immunol.* **2003**, *3*, 710−720.
(31) Torres, A. M.; Kuchel, P. W. The beta-defensin-fold family of polypeptides. *Toxicon* **2004**, *44*, 581−588.
(32) Kem, W. R.; Parten, B.; Pennington, M. W.; Price, D. A.; Dunn, B. M. Isolation, characterization, and amino acid sequence of a polypeptide neurotoxin occurring in the sea anemone Stichodactyla helianthus. *Biochemistry* **1989**, *28*, 3483−3489.
(33) Svensson, B.; Fukuda, K.; Nielsen, P. K.; Bønsager, B. C. Proteinaceous alpha-amylase inhibitors. *Biochim. Biophys. Acta, Proteins Proteomics* **2004**, *1696*, 145−156.
(34) König, V.; Vértesy, L.; Schneider, T. R. Structure of the alpha-amylase inhibitor Tendamistat at 0.93 A. *Acta Crystallogr., Sect. D: Biol. Crystallogr.* **2003**, *59*, 1737−1743.
(35) Vértesy, L.; Oeding, V.; Bender, R.; Zepf, K.; Nesemann, G. Tendamistat (HOE 467), a tight-binding alpha-amylase inhibitor from Streptomyces tendae 4158. Isolation, biochemical properties. *Eur. J. Biochem.* **1984**, *141*, 505−512.
(36) Meyer, B. H.; Müller, F. O.; Kruger, J. B.; Grigoleit, H. G. Inhibition of starch absorption by alpha-amylase inactivator given with food. *Lancet* **1983**, *321*, 934.
(37) Rupp, W.; Grigoleit, H. G.; Grötsch, H. Effect on salivary enzymes of alpha-amylase inhibitor HOE 467. *Lancet* **1983**, *321*, 1103−1104.
(38) Williams, L. K.; Zhang, X.; Caner, S.; Tysoe, C.; Nguyen, N. T.; Wicki, J.; Williams, D. E.; Coleman, J.; McNeill, J. H.; Yuen, V.; Andersen, R. J.; Withers, S. G.; Brayer, G. D. The amylase inhibitor montbretin A reveals a new glycosidase inhibition motif. *Nat. Chem. Biol.* **2015**, *11*, 691−696.
(39) Kaspar, A. A.; Reichert, J. M. Future directions for peptide therapeutics development. *Drug Discovery Today* **2013**, *18*, 807−817.
(40) Studier, F. W. Protein production by auto-induction in high density shaking cultures. *Protein Expression Purif.* **2005**, *41*, 207−234.
(41) Li, C.; Begum, A.; Numao, S.; Park, K. H.; Withers, S. G.; Brayer, G. D. Acarbose rearrangement mechanism implied by the kinetic and structural analysis of human pancreatic alpha-amylase in complex with analogues and their elongated counterparts. *Biochemistry* **2005**, *44*, 3347−3357.
(42) Dieffenbach, C. W.; Dveksler, G. S. *PCR Primer: A Laboratory Manual* 2nd ed.; Cold Spring Harbor Laboratory Press: Cold Spring Harbor, New York, 2003

DOI: 10.1021/acscentsci.5b00399
ACS Cent. Sci. 2016, 2, 154−161